ELSEVIER

Journal of Nuclear Materials 254 (1998) 226–233

journal of nuclear materials

Effect of nitrogen on high temperature low cycle fatigue behaviors in type 316L stainless steel

Dae Whan Kim [a,*], Woo-Seog Ryu [a], Jun Hwa Hong [a], Si-Kyung Choi [b]

[a] *Nuclear Structural Steel (Reactor Mat.) Lab, Advanced Nuclear Materials Development Program, Korea Atomic Energy Research Institute, P.O. Box 105, Yusung, Taejon 305-600, South Korea*

[b] *Department of Materials Science and Engineering, Korea Advanced Institute of Science and Technology, 373-1 Kusung-dong, Yusung-gu, Taejon 305-701, South Korea*

Received 9 June 1997; accepted 24 November 1997

Abstract

Strain-controlled low cycle fatigue (LCF) tests were conducted in the temperature range of RT–600°C and air atmosphere to investigate the nitrogen effect on LCF behavior of type 316L stainless steels with different nitrogen contents (0.04–0.15%). The waveform of LCF was a symmetrical triangle with a strain amplitude of $\pm 0.5\%$ and a constant strain rate of 2×10^{-3}/s was employed for most tests. Cyclic stress response of the alloys exhibited a gradual cyclic softening at RT, but a cyclic hardening at an early stage of fatigue life at 300–600°C. The hardening at high temperature was attributed to dynamic strain aging (DSA). Nitrogen addition decreased hardening magnitude (maximum cyclic stress — first cyclic stress) because nitrogen retarded DSA for these conditions. The dislocation structures were changed from cell to planar structure with increasing temperature and nitrogen addition by DSA and short range order (SRO). Fatigue life was a maximum at 0.1% nitrogen content, which was attributed to the balance between DSA and SRO. © 1998 Elsevier Science B.V.

PACS: 62.20.M

1. Introduction

The reactor vessel and piping of liquid metal reactors (LMR) are subjected to repeated thermal stresses as a result of temperature gradients which occur on heating and cooling during starts-ups and shut-downs. Therefore, resistance to low cycle fatigue (LCF) at high temperature is an essential requirement in the design of LMR components which operate at 600°C. Nitrogen alloyed type 316L stainless steel is a prospective structural material for LMR because nitrogen is known to be beneficial to LCF resistance of type 316L stainless steel. It has been reported [1] that nitrogen alloyed type 316L stainless steels which exhibit planar slip are more resistant to fatigue than type 316L stainless steels with wavy slip. The formation of planar dislocation arrays is generally associated with low stacking fault energy (SFE) and short range order (SRO), which inhibit cross slip [2–5].

The energy for interaction of substitutional elements with nitrogen has been calculated in austenitic stainless steels [6], and the results have shown that chromium and Mn have a strong potential to order with nitrogen, the degree being larger in the case of chromium than Mn. A strong interaction between chromium and nitrogen contributes to form SRO in nitrogen alloyed type 316L stainless steels although no direct experimental evidence is currently available because of the very small scale of SRO [7]. The existence of SRO has been currently identified by the formation of dipole since the dislocation structure shows dipoles in ordered alloys [7,8]. On the other hand, SFE increases with increasing temperature and is not

* Corresponding author. Tel.: +42-868-2441; fax: +42-868-8346; e-mail: kwkim1@nanum.kaeri.re.kr.

PII S0022-3115(97)00360-7

changed by nitrogen content [3,5]. Thus the origin of planar slip in nitrogen alloyed type 316L stainless steel is due to SRO rather than SFE at high temperature since SRO is independent of temperature [1,4,8–10].

Dynamic strain aging occurs at high temperature low cycle fatigue test in austenitic stainless steel [11–13]. Under the influence of DSA, the higher response stress developed during cyclic deformation can lead to a large stress concentration at the crack tip, which would account for increased crack growth rates and hence a reduced number of cycles in the crack propagation stage, namely, DSA decreases fatigue life at high temperature. It was reported [14] that nitrogen retarded DSA since nitrogen increased the activation energy for DSA. Thus the increase of fatigue life at high temperature may be related with DSA. But the mechanism that nitrogen affects the high temperature fatigue life was mainly studied in the viewpoint of SRO rather than DSA [8,9,15,16]. Therefore, the increase of fatigue life at high temperature in nitrogen alloyed type 316L stainless steel should be investigated from the viewpoint of DSA in addition to SRO but this has not been studied systematically. The purpose of this study is to clarify the relation between the increase of fatigue life and DSA at high temperature in nitrogen alloyed stainless steel.

2. Experimental

Laboratory ingots containing four different levels of nitrogen were prepared by vacuum induction melting (VIM). The chemical compositions and grain sizes were given in Table 1. All four alloys were solution treated at 1100°C for 1 h and water quenched. The grain size of alloys was determined in the range of 100–47 μm from the method of line intersections. LCF test specimens were taken as rolling direction and machined to cylindrical with 8 mm gage length and 7 mm diameter as shown in Fig. 1. The gage sections of the specimens were polished using a 1000 grit sand paper with strokes along the specimen axis.

LCF tests were carried out in air environment under fully reversed axial strain control mode using an Instron 8562 model. Strain gage with quartz rod was directly attached to the shoulder of specimen by punching quartz rod to marks since stress localization and fracture might occur at this punched sites if the punched sites were in the gage length. Strain change in the 8 mm gage length was calibrated using the 25 mm strain gage for high temperature. The waveform was triangular with a total strain of 1%, and the strain rate was 2×10^{-3}/s for most tests. The test temperature was in the range of RT–600°C and temperature was maintained constantly within ±2°C during the period of the test. All specimens were held at the test temperature for 1 h before starting the test. The fatigue life was defined to be the number of cycles corresponding to 25% reduction in saturation stress. Dislocation structures of specimens after testing were examined using transmission electron microscopy (TEM) of JEOL 2000FX operating at an acceleration voltage of 200 keV. The thin foils for examination were cut perpendicular to the loading axis at a distance of 1 mm away from the fractured surfaces and then electropolished in a solution containing 5% perchloric acid and 95% acetic acid at 70 V and 10°C.

Table 1
Chemical composition of four experimental melts (wt%)

Spec. ID	C	Si	Mn	Ni	Cr	Mo	N	Fe	Grain size (μm)
N04	0.018	0.67	0.95	12.21	17.78	2.36	0.042	Bal.	100
N10	0.019	0.70	0.97	12.46	17.23	2.38	0.103	Bal.	47
N13	0.019	0.70	0.96	12.45	17.17	2.39	0.131	Bal.	47
N15	0.020	0.67	0.96	12.19	17.88	2.41	0.151	Bal	78

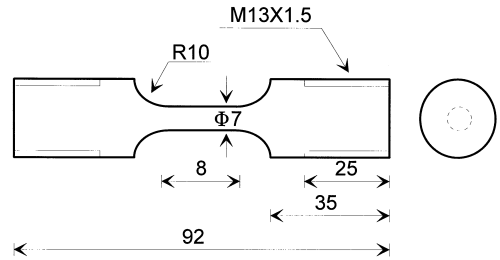

Fig. 1. Geometry of low cycle fatigue specimen (unit is mm).

3. Results and discussion

3.1. Hardening behavior at an early stage of fatigue life

The cyclic stress responses at each temperature in type 316L stainless steels with different nitrogen content were illustrated in Fig. 2. There were three kinds of responses with temperature: gradual softening at RT, hardening at an early stage followed by softening and saturation at 300–400°C, and hardening followed by saturation at 500–600°C. Hardening magnitude (hardening stress) was calculated from the difference between maximum and first cyclic stresses (maximum cyclic stress — first cyclic stress) at an early stage of fatigue life. The degree of hardening magnitude increased with increasing temperature as shown in Fig. 3.

Since hardening occurred at high temperature rather than RT the possible hardening mechanisms are temperature-dependent processes such as precipitation of second phases and aging (especially dynamic strain aging) rather than dislocation production because dislocation density decreases with increasing temperature. Carbides such as $M_{23}C_6$ and M_6C precipitate after about 50 h at 600°C in

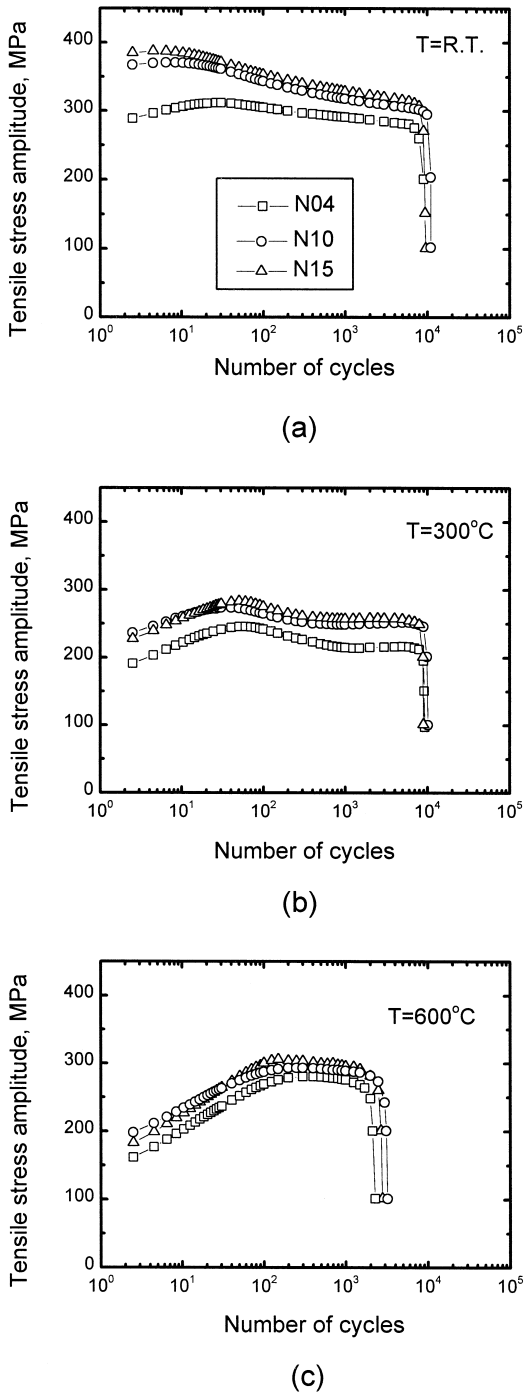

Fig. 2. Cyclic stress response for nitrogen alloyed type 316L stainless steels at temperature of (a) RT, (b) 300°C, and (c) 600°C.

type 316L stainless steels [17] and nitrogen addition retards the precipitation of carbides [18]. Cr_2N precipitations in the nitrogen alloyed austenitic stainless steels have been reported in steels containing greater than 0.16 wt% nitrogen according to atom probe field ion microscopy [19], TEM [20,21], and extended X-ray absorption fine structure [22]. The time for this LCF tests, however, was less than 5 h at 600°C. Since plastic deformation may accelerates precipitation of carbides and nitrides they were observed from TEM examinations in specimens LCF tested at 600°C. Carbides and nitrides were not observed in these test conditions. Thus precipitation of carbides and nitrides were eliminated from the cyclic hardening mechanisms in these test conditions. So, the hardening may be ascribed to DSA. According to tensile test results [14], DSA was observed in

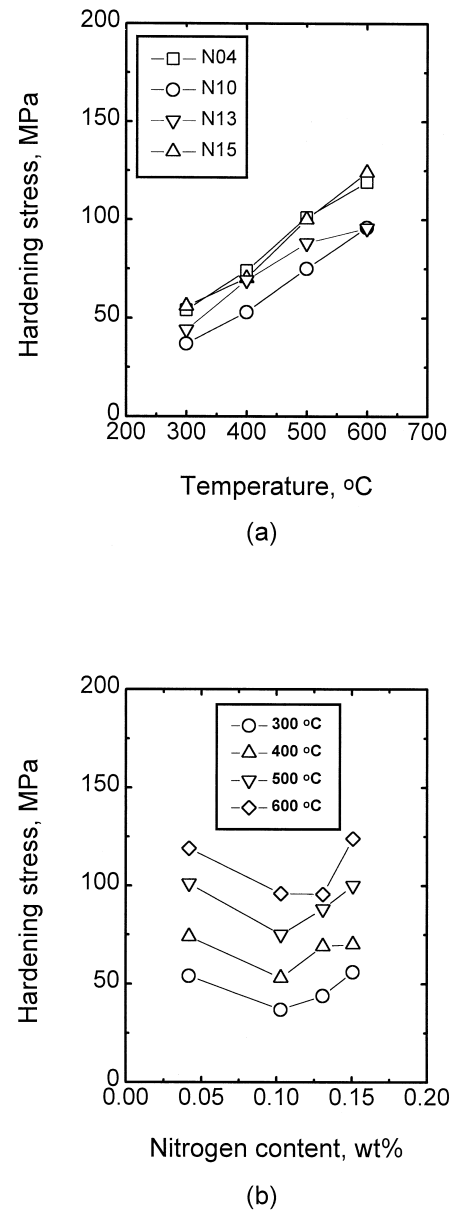

Fig. 3. Cyclic hardening stress (maximum cyclic stress-first cyclic stress) with (a) temperature and (b) nitrogen content.

the temperature range of 400–650°C in type 316L stainless steel with 0.01% and 0.1% nitrogen content. Tsuzaki et al. [23] observed that serrations began in the saturated stress stage of fatigue process under various strain rate and temperature in type 304 stainless steel. They proposed that, in the saturated stress stage, dislocations move with a shuttling motion between cell walls. Such a dislocation motion is different from that in monotonic tensile deformation. At the position of maximum tensile stress in the hysteresis loop of fatigue deformation, the mobile dislocations pile up against the cell wall. When compressive stress is applied, the dislocations move in a reverse manner and pile up against the cell wall on the opposite side. In such a process the dislocations are arrested at the cell wall for the period of half a fatigue cycle. Therefore, on the assumption used in McCormick's model [24] the arrest time of a dislocation in the saturated stress stage of the fatigue process can be expressed in terms of the strain rate $\dot{\varepsilon}$ and the total strain range $\Delta\varepsilon_t$ as

$$t_w = \frac{\Delta\varepsilon_t}{\dot{\varepsilon}}. \quad (1)$$

It was emphasized that t_w in fatigue deformation is much larger than t_w in monotonic deformation. It was thus considered that this longer arrest time due to cell shuttling motions of dislocations is associated with the lower critical temperature for DSA for fatigue deformation than critical temperature for monotonic deformation. Thus, the critical temperature for the onset of serrations during fatigue deformation was much lower than that during monotonic tensile deformation with various strain rate and temperature range. Considering these results, the temperature range showing cyclic hardening in LCF test was consistent with the temperature range for DSA.

The phenomenon of serrated yielding is often a manifestation of DSA but serration was not shown in hysteresis loop in this LCF tests. Theoretical models [24,25] of the DSA phenomenon have presented explanation in terms of the interaction between moving dislocations and diffusing solute atoms. The mobility of solute atoms capable of segregating on dislocations temporarily arrested at localized obstacles is a central feature of such models. It is known that solute atom for DSA is chromium at high temperature in type 316L stainless steel [26]. Whereas the resistance of localized obstacles to dislocation motion decreases in a thermally activated process, the glide resistance increases if solute segregation is to become operative during the arrest time. The net result of the competition of these two factors makes strain rate sensitivity, $d\sigma/d\dot{\varepsilon}$, be a negative in DSA temperature range [27]. LCF tests were conducted for N04 specimens at three different strain rate of 1×10^{-2}/s, 2×10^{-3}/s, and 2×10^{-4}/s and 600°C. Cyclic tensile stress amplitude increased and fatigue life decreased with decreasing strain rate as shown in Fig. 4, which was indicative for the negative of strain rate sensitivity. Therefore, it is considered that DSA occurred in LCF tests at 600°C although serrations were not shown in hysteresis loop.

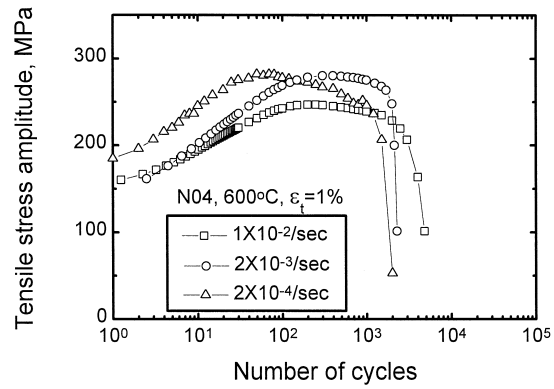

Fig. 4. Effect of strain rate on low cycle fatigue behaviors for N04 at 600°C.

Fig. 5 shows dislocation structures after LCF tests. When nitrogen was not added, cell structures and cell wall dislocation arrangements, which was an efficient low energy means of storing the appropriate dislocation density, were formed at RT but dislocation structure changed from cell to planar with increasing temperature. Kanazawa et al. [28] have analyzed that the dislocation substructure changed from wavy to more planar in the temperature range occurring DSA and became wavy again at higher temperatures in type 310 stainless steels. Microstructure change from cell to planar in this study is consistent with Kanazawa's results. From these results the hardening behavior at an early stage of fatigue life is due to DSA.

3.2. Fatigue life behavior with temperature

In Fig. 6, fatigue life decreased drastically at 300–600°C which was consistent with the temperature range for DSA. This result implies that fatigue life is related with DSA. The higher response stress developed during cyclic deformation under the influence of DSA can lead to a large stress concentration at the crack tip and increases crack growth rates [11]. So, it is considered that the decrease of fatigue life at high temperature is due to DSA.

Dynamic recovery occurs at high temperature but nitrogen hinders dynamic recovery since nitrogen induces planar slip and hinders cross slip. Fatigue life increased up to 0.1% nitrogen content and decreased at 0.15% nitrogen content as shown in Fig. 6. Dynamic recovery behavior is not consistent with fatigue life behavior. So, fatigue life is dependent on DSA rather than dynamic recovery.

The martensite formed in the surface layers of the specimen acts as the preferential sites of crack nucleation and also enhances the fatigue crack growth rate by increasing the stress amplitude. Both these effects could lead to reduction in fatigue life. So, the lesser the martensite

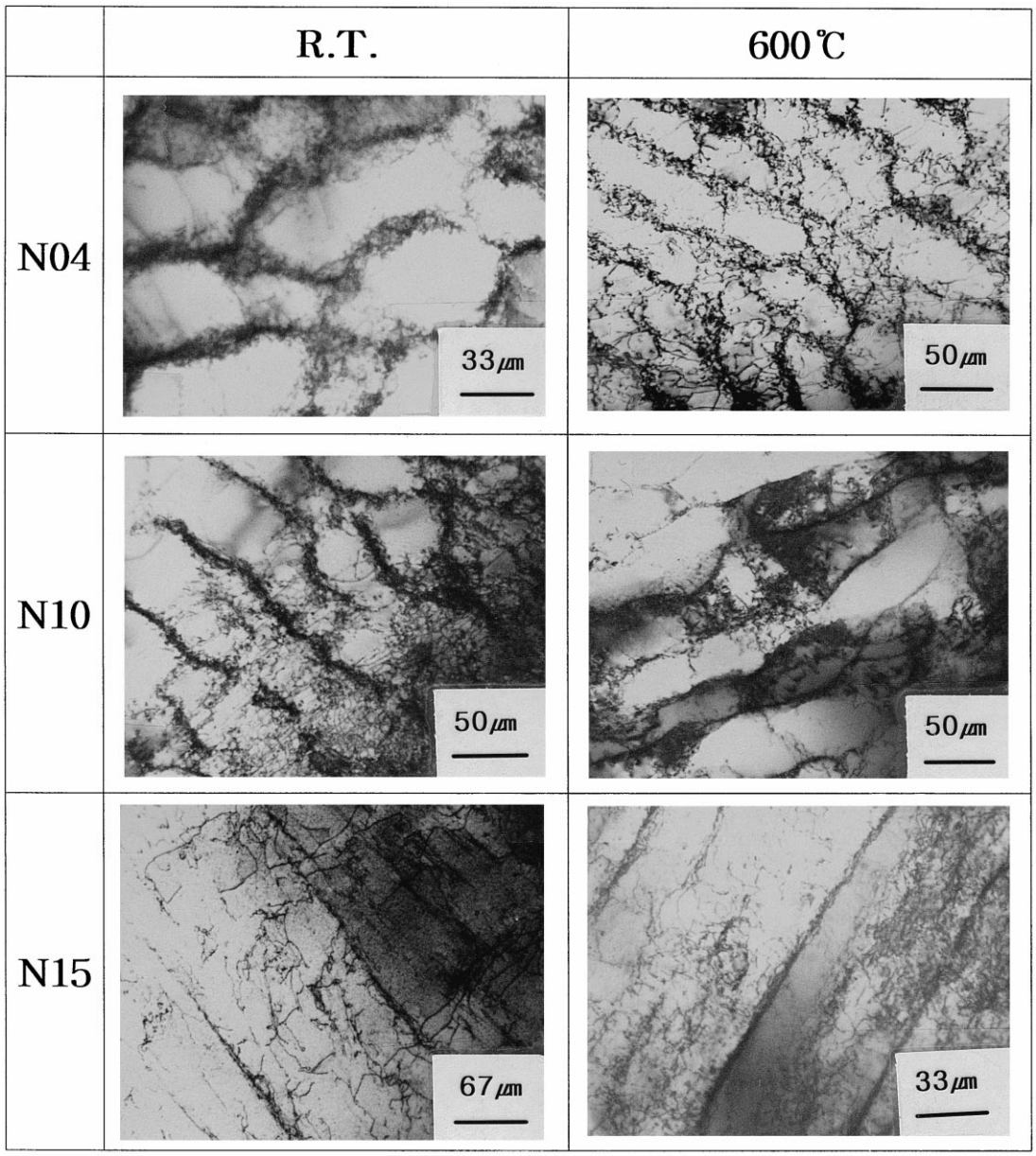

Fig. 5. Dislocation structures after LCF testing at RT and 600°C for (a) N04, (b) N10, and (c) N15.

formed the longer the fatigue life was. Nitrogen prevents formation of martensite during cyclic straining since nitrogen is an austenite stabilizer. The effect of martensite transformation on LCF life can be neglected at high temperature LCF test condition such as this study since martensite transformation decreases with increasing temperature.

LCF life may be also affected by oxidation which occurs in the temperature range for DSA. Many mechanisms about the effect of oxidation on LCF life were suggested [29–31]. Microcracks formed at the oxidation layers of specimen surface make local stress and assist the initiation of fatigue crack. Fatigue crack growth rates increase since matrix composition is changed by the formation of oxide. Oxygen makes grain boundary become brittle and fatigue cycles for crack initiation decrease by surface oxide and fatigue crack growth rate increases due to the brittle oxide layer of crack tip. The decrease of fatigue life at 300–600°C might be due to DSA and oxidation but Srinivasan et al. [11] reported that a drastic reduction in fatigue life above 300°C was due to DSA effect.

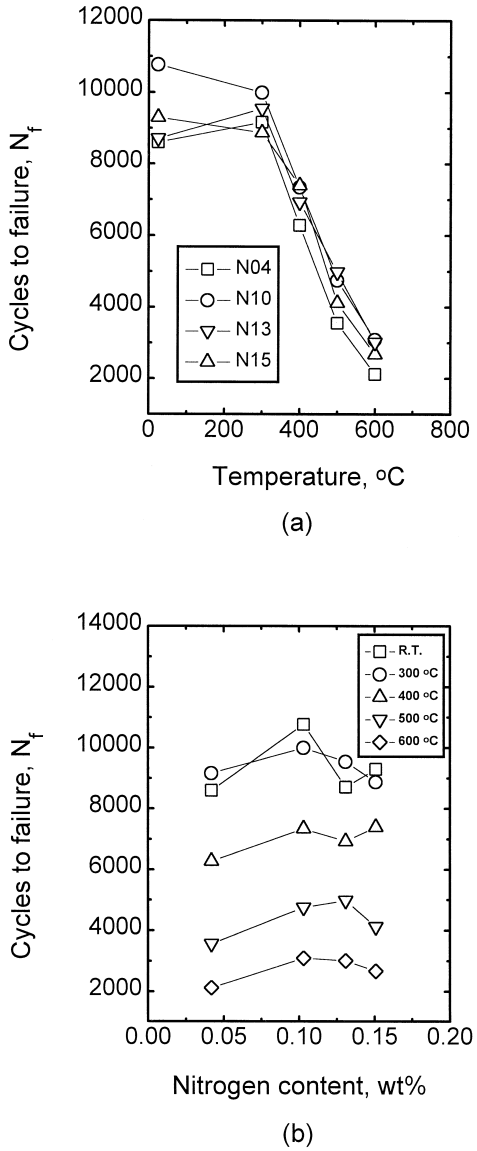

Fig. 6. Low cycle fatigue life with (a) temperature and (b) nitrogen content.

3.3. Nitrogen effect on LCF behaviors

Maximum and saturation stress increased with nitrogen content as shown in Fig. 2. The contribution of nitrogen to the strengthening of austenitic stainless steels is made up of two components: one is a thermal component due to solid–solution strengthening, which is proportional to $N^{1/2}$, and the other is an athermal component attributed to SRO, which is proportional to N, and/or grain size strengthening due to grain refinement [7,32–34]. The thermal component is very strong at temperatures below ambient but weak at temperatures above 300°C. Carbon strengthening of austenitic stainless steels is suggested due to the presence of chromium carbon or carbon vacancy clusters [35,36]. However, nitrogen strengthening cannot be explained by the presence of clusters containing nitrogen according to the clear evidence of planar slip [7]. The most rational explanation of the nitrogen strengthening seems to be SRO due to the unusually strong affinity between chromium and nitrogen. In addition, nitrogen also has an effect on grain size strengthening since grain size decreased with nitrogen addition. Since SRO and nitrogen-enhanced grain size strengthening do not change markedly with temperature [37,38], these mechanisms are responsible for high temperature strengthening in nitrogen alloyed type 316L stainless steel.

TEM examination in nitrogen alloyed steels after LCF tests has shown well developed planar slip bands [1,7,11,32] instead of cells at both RT and 600°C as shown in Fig. 5. The planar slip has been explained by SRO [4] as follows: dislocations moving through the lattice are arrested and piled up at SRO. The higher stress for more plastic deformation will destroy SRO and when a dislocation source is activated successive dislocations will move easier so that they will tend to remain in the same slip plane rather than cross slip. Taillard and Foct [16] reported that the motion of the dislocations is controlled by their SRO interaction at RT since the magnitude of the friction stress is clearly higher than that of the back stress component and reverse stress does not restore SRO since friction stress decreases with increasing cycles.

Because the hardening at an early stage of fatigue life was attributed to DSA and DSA was based on the chromium diffusion to dislocations, chromium diffusivity was measured as function of nitrogen content by microanalysis of chromium depleted zones using analytical electron microscopy in nitrogen alloyed type 316L stainless steels sensitized for 100–200 h at 650°C. The volume diffusion coefficients for chromium were determined from the chromium profiles obtained for each steel by using the method suggested by Doig and Edington [39]. The following solution of Fick's second law for diffusion can be used to describe the chromium distribution obtained experimentally perpendicular to grain boundaries:

$$\frac{C_x - C_0}{C_1 - C_0} = \mathrm{erf}\left(\frac{x}{2\sqrt{Dt}}\right), \tag{2}$$

where C_x is the matrix composition at distance x from the grain boundary, C_0 is the experimentally determined equilibrium chromium concentration at the boundary, C_1 is the chromium concentration in the bulk, D is the volume diffusion coefficient for chromium, and t is the aging time. The D value is then calculated from the experimental chromium profiles by first determining the concentration (C_x) for each steel, at which the term $x/(2\times\sqrt{D\times t})$

Table 2
Chromium diffusion coefficient at 650°C in nitrogen alloyed type 316L stainless steels

Spec. ID	D_{cr} (m^2/s)
N04	2.7×10^{-20}
N10	1.7×10^{-20}
N15	1.3×10^{-20}

in error function of Eq. (2) is equal to unity, as shown in Eq. (3):

$$\frac{C_x - C_0}{C_1 - C_0} = \mathrm{erf}(1) = 0.84. \quad (3)$$

The distance from the grain boundary (x) at which the calculated C_x value is obtained is then inserted into Eq. (4) to determine the volume diffusion coefficient of chromium:

$$D = \left(\frac{X}{2}\right)^2 \frac{1}{t}. \quad (4)$$

The measured chromium diffusion coefficients were summarized in Table 2. Nitrogen decreased the chromium diffusivity. Tensile test [14] indicated that the temperature range for DSA was shifted to higher temperature by nitrogen addition in type 316L stainless steels. Namely, nitrogen retards DSA. This result is consistent with the fact that nitrogen decreases chromium diffusivity.

From the Fe–N phase diagram 0.15% nitrogen content can be solid dissolved completely. The strong interaction between chromium and nitrogen forms SRO. Byrnes et al. [7] explained the athermal flow stress of the stable austenitic alloys increased linearly with increasing nitrogen concentration since SRO is linearly related to the nitrogen concentration. It was expected that fatigue life would increase with adding nitrogen at high temperature since SRO formed by the interaction between chromium and nitrogen forms planar slip and nitrogen retards DSA. But fatigue life increased up to 0.1% nitrogen content and decreased at 0.15% nitrogen content as shown in Fig. 6. And the hardening stress decreased up to 0.1% nitrogen content and increased above 0.1% nitrogen content. Since the reduction of fatigue life is due to DSA and the hardening stress results from DSA fatigue life behaviors are related with the hardening behaviors. Chromium diffusivity and DSA decreases with adding nitrogen but SRO, which acts as obstacle for moving dislocations, increases DSA [4] since SRO increases linearly with adding nitrogen. At low nitrogen content chromium diffusivity is a main mechanism for DSA since the number of obstacles (SRO) are low and chromium diffusivity is high, while SRO is a main mechanism for DSA since the number of obstacles (SRO) are high and chromium diffusivity is low at high nitrogen content. So, DSA was minimum at 0.1% nitrogen content since the number of obstacle (SRO) and chromium diffusivity are not high. From these behaviors fatigue life behaviors at high temperature are consistent with hardening behaviors, namely DSA behaviors. So, fatigue life was maximum at 0.1% nitrogen content since hardening is minimum at 0.1% nitrogen content due to the balance between SRO and DSA with nitrogen content.

Fatigue failure is composed of two process such as crack nucleation and crack propagation. Fatigue life may increase also with decreasing grain size in planar slip mode in addition to SRO and DSA since crack nucleation is strongly dependent on grain size and inhibited by decreasing grain size [40]. Maximum crack depth from surface decreased with adding nitrogen at RT since planar slip results from SRO and slip reversibility increases in nitrogen alloyed steel. But maximum crack depth from surface does not decreases with adding nitrogen at high temperature since cross slip and DSA increases and slip reversibility decreases with increasing temperature [41]. So, it is considered that crack propagation rather than crack nucleation is a main mechanism at high temperature LCF in nitrogen alloyed steel since nitrogen decreases fatigue crack growth rate but does not decrease maximum crack depth at high temperature [41,42]. Thus the increase of fatigue life at high temperature with adding nitrogen is due to retardation of DSA which increases the fatigue crack growth rate rather than decrease of grain size which decreases crack nucleation. This result is consistent with the fact that fatigue crack growth rate decreases with adding nitrogen [42].

4. Conclusions

Strain-controlled LCF tests were conducted in air between RT–600°C to investigate the nitrogen effect on LCF behaviors of type 316L stainless steels with different nitrogen contents (0.04–0.15%). The test results are concluded as follows.

(1) Cyclic hardening at an early stage of fatigue life in the temperature range of 300–600°C rather than RT was shown. This behavior was attributed to DSA. The occurrence of DSA was identified from the results that strain rate sensitivity was negative, the hardening stress increased with temperature, dislocation structure changed from cell to planar, and the temperature range for DSA was identical to the temperature range of cyclic hardening.

(2) Nitrogen decreased chromium diffusion coefficient.

(3) Fatigue life increased with adding nitrogen at high temperature since nitrogen retarded DSA.

References

[1] J.O. Nilsson, Scr. Metall. 17 (1983) 593.
[2] R.P. Reed, J. Met. (1989) 16.

[3] V. Gerold, H.P. Karnthaler, Acta Metall. 37 (8) (1989) 2177.
[4] D.L. Douglass, G. Thomas, W.R. Roser, Corros. NACE 20 (1964) 15t.
[5] P.R. Swann, Corrosion 19 (1963) 1021.
[6] K. Shibata, Y. Kishimoto, N. Namura, T. Fujita, ASTM STP 857 (1985) 31.
[7] M.L.G. Byrnes, M. Grujijic, W.S. Owen, Acta Metall. 35 (7) (1987) 1853.
[8] J.B. Vogt, S. Degallaix, J. Foct, Int. J. Fatigue 6 (4) (1984) 211.
[9] R. Taillard, Proc. Conf. on Low Cycle Fatigue and Elasto-Plastic Behavior of Materials, 1987, Elsevier, Amsterdam, 1987, p. 83.
[10] J.B. Vogt, J. Foct, C. Regnard, G. Robert, J. Dhers, Metall. Trans. 22A (1991) 2385.
[11] V.S. Srinivasan, R. Sandhay, B.S. Rao, S.L. Mannan, K.S. Raghavan, Int. J. Fatigue 13 (6) (1991) 471.
[12] J.T. Barnby, J. Iron Steel Inst. (1965) 392.
[13] S.L. Mannan, K.G. Samuel, P. Rodriquez, Trans. Ind. Inst. Metals 4&5 (1983) 313.
[14] D.W. Kim, W.S. Ryu, J.H. Hong, S.K. Choi, J. Mater. Sci. (1997), to be published.
[15] J.O. Nilsson, Fatigue Eng. Struct. 7 (1) (1984) 55.
[16] R. Taillard, J. Foct, Proc. Int. Conf. on High Nitrogen Steels, Lille, France, May 18–20, 1988, The Institute of Metals, 1989, p. 387.
[17] D. Pecker, I.M. Bernstein, Handbook of Stainless Steels, McGraw-Hill, New York, 1977.
[18] F.B. Pickering, Proc. Int. Conf. on High Nitrogen Steels, Lille, France, May 18–20, 1988, The Institute of Metals, London, 1989, p. 30.
[19] G. Wahlberg, U. Rolander, H.O. Andren, Proc. Int. Conf. on High Nitrogen Steels, Lille, France, May 18–20, 1988, The Institute of Metals, London, 1989, p. 163.
[20] E. Ruedl, G. Valdre, J. Mater. Sci. 23 (1988) 3698.
[21] E. Ruedl, G. Valdre, P. Dealvignette, U. Valdre, Phys. Status Solidi (a) 107 (1988) 745.
[22] K. Oda, N. Kondo, K. Shibata, ISIJ Int. 30 (1990) 625.
[23] K. Tsuzaki, T. Hori, T. Maki, I. Tamura, Mater. Sci. Eng. 61 (1983) 247.
[24] P.G. McCormick, Acta Metall. 20 (1972) 351.
[25] A.H. Cottrell, Philos. Mag. 44 (1953) 829.
[26] S. Venkadesan, C. Phaniraj, P. Rodriguez, Acta Metall. 40 (3) (1992) 569.
[27] A. Van den Beukel, Phys. Status Solidi (a) 30 (1975) 197.
[28] K. Kanazawa, K. Yamaguchi, S. Nishijima, ASTM STP 942 (1988) 519.
[29] H. Teranishi, A.J. Mcevily, Metall. Trans. 10 (1979) 1806.
[30] D.J. Dugette, M. Gell, Metall. Trans. 2 (1971) 1325.
[31] L.F. Coffin Jr., Metall. Trans. 3 (1972) 1777.
[32] L.Å. Norström, Met. Sci. (1977) 208.
[33] E. Werner, Mater. Sci. Eng. A 101 (1988) 93.
[34] A. Soussan, S. Degallaix, T. Magnin, Mater. Sci. Eng. A 142 (1991) 169.
[35] K.S.B. Rose, S.G. Glover, Acta Metall. 14 (1966) 1505.
[36] C.F. Jenkins, G.V. Smith, Trans. Metall. Soc. A.I.M.E. 245 (1969) 2149.
[37] J.W. Simmons, Mater. Sci. Eng. A 207 (1966) 159.
[38] J. Rawers, M. Grujicic, Mater. Sci. Eng. A 207 (1996) 188.
[39] P. Doig, J.W. Edington, Philos. Mag. 28 (1973) 961.
[40] F.-L. Liang, C. Laird, Mater. Sci. Eng. A 117 (1989) 95.
[41] D.W. Kim, W.S. Ryu, J.H. Hong, S.K. Choi, Proc. 11th Conf. on Mechanical Behaviors of Materials, Seoul, Korea, 22 August, S.K. Hur, J.H. Hong (Eds.), The Korean Institute of Metals and Materials, 1997, p. 229.
[42] J. Dhers, J. Foct, L.B. Vogt, Proc. Int. Conf. on High Nitrogen Steels, Lille, France, May 18–20, 1988, The Institute of Metals, London, 1989, p. 199.